Estuarine Mixing Drives Organic Nitrogen Transformation and Bioavailability Dynamics

Chenglong Han[1], Shaojun Qiu[1], Xinyi Li[1], Ying Ke[1], Rolf D. Vogt[2], Xueqiang Lu[1]

[1]Tianjin Key Laboratory of Environmental Technology for Complex Trans-media Pollution, Tianjin International Joint Research Center for Environmental Biogeochemical Technology, College of Environmental Science and Engineering, Nankai University, Tianjin 300350, China
[2]Norwegian Institute for Water Research, Oslo 0579, Norway

Correspondence to: Xueqiang Lu (luxq@nankai.edu.cn)

Abstract. Estuaries act as critical transition zones for nitrogen transport, where the dynamics of inorganic nitrogen have been extensively studied. In contrast, organic nitrogen (ON), encompassing particulate organic nitrogen (PON) and dissolved organic nitrogen (DON), is strongly influenced by estuarine mixing of freshwater and seawater. However, the mechanisms driving ON transformation and their implications for bioavailability remain poorly understood. Here, estuarine mixing experiments are conducted across salinity gradients to explore ON transformation and changes in nitrogen bioavailability driven by physicochemical and biological processes. Using tangential flow filtration, optical signatures, and stable isotopes ($\delta^{13}C$, $\delta^{15}N$), we quantified ON composition and molecular characteristics. DON dominated the ON pool (> 71%) throughout the mixing process, with the low-molecular-weight (LMW) fraction accounting for 49 ± 7.8%. The results suggest that estuarine mixing drives two co-occurring ON transformation processes with distinct consequences for nitrogen fate. First, salt-induced flocculation and adsorption (i.e. physicochemical processes) preferentially transferred a large fraction (63 ± 11%) of humic-like components, mainly terrestrial refractory compounds, into the particulate phase, thereby increasing PON. The isotopic enrichment ($\delta^{13}C$, $\delta^{15}N$) and elevated C/N ratios in PON further suggested the re-adsorption of biologically modified and $\delta^{15}N$-enriched DON onto particles, enhancing PON refractoriness. Second, biological activity promoted the degradation of residual humic-like components (especially microbial C3), producing labile LMW-DON and ammonium; a strong negative correlation between humic-like and protein-like fluorescence in control treatments evidenced this conversion. Overall, estuarine mixing generates a dual response: physicochemical processes channel humic-like ON into refractory particulate pools, while biological processing simultaneously shifts the residual dissolved pool toward a more labile composition. This mechanistic framework advances our understanding of non-conservative ON behavior across estuarine salinity gradients and has implications for assessing nitrogen bioavailability in receiving coastal waters.

1 Introduction

Estuaries are critical transitional zones between rivers and the sea that critically mediate the flux of nitrogen to the sea (Kellerman et al., 2014; Wan et al., 2023; Wu et al., 2023). Globally, rivers deliver an estimated 36–60 Tg N yr^{-1} to coastal

waters, including approximately 11.8 Tg N yr^{-1} as dissolved organic nitrogen (DON), highlighting the substantial role of organic nitrogen in land–ocean nitrogen transfer (Mayorga et al., 2010; Tivig et al., 2021). Recent global modeling further suggests that riverine total nitrogen export to the ocean increased from 27.5 Tg N yr^{-1} in 1901–1920 to 40.0 Tg N yr^{-1} in 1995–2014, with DON export increasing by 50.6%, emphasizing the growing importance of estuarine ON transformation under global environmental change (Ma et al., 2025). While dissolved inorganic nitrogen (DIN) has been extensively studied (Cai et al., 2000; Zhou et al., 2023; Tang et al., 2024, 2025), organic nitrogen (ON) remains less understood, despite often constituting the majority (greater than 50%) of the total nitrogen pool (Berman and Bronk, 2003; Jani and Toor, 2018; Yan et al., 2024). ON is operationally fractionated into particulate (PON) and dissolved (DON) forms (Bronk et al., 2007; Yan et al., 2021). Recent advancements, such as tangential flow filtration (TFF), further separate DON into high-molecular-weight colloidal (CON) and low-molecular-weight truly dissolved (tDON) fractions (Edokpa et al., 2018; Rostad et al., 1997; Xu et al., 2018). These techniques enable detailed investigations into the physicochemical behavior and microbial bioavailability of different ON pools (Pan et al., 2020; Xu et al., 2018; Fagerberg et al., 2009; Li et al., 2020; Seitzinger et al., 2002). Given that excessive export of terrestrial ON can drive coastal eutrophication and hypoxia, understanding the transformation and fate of these distinct ON fractions in estuaries is a scientific priority.

In estuaries, salinity gradients drive complex biological and physicochemical processes that govern the fate of ON (Jani and Toor, 2018; Zhang et al., 2022; Wu et al., 2023). Recent studies have shown that DON is considered as a bioavailable nitrogen source for phytoplankton and bacteria in coastal waters (Bronk et al., 2007; Jani and Toor, 2018; Yan et al., 2021). Contrary to early models of conservative dilution mixing, in which solute concentrations vary linearly with salinity between the freshwater and seawater end-members (i.e., following the theoretical dilution line) (Langmuir et al., 1978; Officer, 1979), ON behavior is often non-conservative, with measured concentrations deviating above (net addition) or below (net removal) the theoretical dilution line. This results from the interplay of biological processes (e.g., microbial degradation, uptake) and physicochemical removal mechanisms (e.g., adsorption, flocculation) (Jani and Toor, 2018; Yan et al., 2022; Zhou et al., 2016). While biological activity alters ON's chemical characteristics, physicochemical processes can transfer it to the particulate phase (Zhou et al., 2021; Yan et al., 2023; Li et al., 2024). However, how and what these processes interact and collectively determine the net transformation and bioavailability of the ON pool remains a critical knowledge gap.

Given the complex structure of DON and its compositional overlap with a significant proportion of dissolved organic matter (DOM), ultraviolet-visible spectroscopy (UV-Vis) and Excitation-emission matrix - Parallel factor analysis (EEM-PARAFAC) were used to characterize DON (Hounshell et al., 2017; Li et al., 2024). Humic-like (terrestrial and microbial sources) and protein-like components are considered as the dominant terrestrial DON components entering the sea (Stedmon and Markager, 2005; Yan et al., 2024). The terrestrial humic-like components, characterised with complex and high molecular weight and lower bioavailability, are preferentially removed through polymerization (Asmala et al., 2014; Pan et al., 2020; Shimabuku et al., 2017), while microbial humic-like components could be partially utilized by organisms (Cole et al., 2007; Yao et al., 2024). Moreover, protein-like components, featured low-molecular-weight, are more easily utilized by microorganisms (Li et al., 2017; Zhang et al., 2015; Zhang et al., 2024), thereby promoting microbial activity. Research

shows a significant correlation between DON bioavailability and protein-like fluorescence, and the latter could be used as an alternative means to estimate the bioavailability of the DON pool (Hu and Ren, 2016; Li et al., 2019). Despite these advances, limitations remain in understanding how different DON components respond to the interplay of physicochemical and biological processes across the estuarine salinity gradient, and how these transformations influence their bioavailability.

The stable isotopic composition of PON (δ^{15}N-PON) is widely used to trace its sources and behavior (Kodama et al., 2021; Zhu et al., 2021). Similar to DON, PON exhibits non-conservative behavior in estuaries due to continuous physicochemical and biological alterations (Wu et al., 2016; Dähnke et al., 2022; Ghosh et al., 2024). Consequently, the δ^{15}N-PON signature reflects not only its source but also subsequent transformations, such as isotopic fractionation during nitrate assimilation or DON utilization, which can alter the δ^{15}N of the residual nitrogen pool (Yan et al., 2021). Although combining fluorescence and isotopic techniques has advanced our understanding of ON dynamics (Yan et al., 2022; Yao et al., 2024; Zhong et al., 2022), a framework linking these transformations to ecological outcomes (e.g., algal blooms) is lacking. Specifically, the relative importance of biological versus physicochemical processes in regulating the overall fate of ON across estuarine gradients remains a key uncertainty. Here, we address this gap by isolating and quantifying coupled physicochemical–biological pathways that directly alter ON partitioning and bioavailability during mixing, providing mechanistic constraints that can be evaluated against field gradients and incorporated into estuarine nitrogen budget models.

In this study, estuaries are considered not merely as a passive "nitrogen filter", but rather as an active "nitrogen transformer", where complex processes jointly shape the cycling pathways of ON. Accordingly, this study aims to investigate the roles of biological and physicochemical processes in driving the transformation and bioavailability of ON during estuarine mixing. To this end, estuarine mixing experiments were conducted across salinity gradients under two treatments: biologically active mixing (BAM; combined processes) and biologically inhibited mixing (BIM; physicochemical processes only). Tangential flow filtration, ON content, optical characteristics, and δ^{13}C and δ^{15}N isotopes were analyzed to elucidate the mechanisms controlling ON fate and its impact on coastal nitrogen cycling.

2 Materials and methods

2.1 Sampling

River water (salinity = 0.49 PSU) and seawater (salinity = 31.52 PSU) (Table S1) were collected in July 2024 using polyethylene containers from the Ziya Xinhe River (117.25°E, 38.60°N), and from Bohai Bay, China (118.18°E, 38.66°N), approximately 40 km downstream of the river mouth, respectively (Fig. S1). Phytoplankton biomass typically peaks during summer in the study area, increasing both the concentration and molecular complexity of DON in its riverine and marine environments. Water temperature, salinity, pH, and dissolved oxygen (DO) were measured using a portable multiparameter analyzer (YSI ProPlus, USA) and the values were reported in Table S1. Samples were promptly transported to the laboratory, stored at low temperature in the dark, and homogenized prior to analysis. Additional physicochemical background

information, including nutrient concentrations, suspended particulate matter (SPM), and its mineral composition, is also presented in Table S1.

2.2 Experiments

River water and seawater were mixed at the following seven volume ratios (v/v) to prepare 5 L of solution: 10:0, 8:2, 6:4, 5:5, 4:6, 2:8, and 0:10. Two experimental treatments were performed. These ratios were selected to span the full salinity gradient with finer resolution in the low-to-mid salinity range, where non-conservative behavior is most pronounced in estuarine systems, and are consistent with mixing designs adopted in previous estuarine simulation studies (Sholkovitz, 1976; Schneider et al., 2016). Biologically active mixing (i.e., biological and physicochemical processes occurring concurrently, BAM): untreated mixtures to assess biological and physicochemical processes. Biologically inhibited mixing (i.e., physicochemical processes only, BIM): mixtures amended with 0.1% (v/v) chloroform to inhibit biological activity and isolate physicochemical processes. All treatments were performed in triplicate. Both treatments were incubated for 3 days under a 12-hour light/12-hour dark cycle at 20°C with agitation at 180 rpm. After incubation, samples were vacuum-filtered through pre-combusted (450 °C, 4 h) 0.45 μm GF filters to separate PON from DON. The filtrate (< 0.45 μm) was subsequently fractionated by tangential flow filtration (TFF) into colloidal (CON; 1 kDa–0.45 μm; also referred to as the high molecular weight (HMW) fraction) and truly dissolved (tDON; < 1 kDa; also known as the low-molecular-weight (LMW) fraction) fractions. TFF was performed in two sequential steps (10 kDa followed by 1 kDa membranes) to reduce membrane fouling and improve permeate flux during the 1 kDa ultrafiltration; the two retentate fractions (>10 kDa and 1–10 kDa) were then pooled as CON, following the conventional operational definition of estuarine colloidal organic matter (Guo and Santschi, 1997; Yang et al., 2021). Further TFF details are provided in Text S1 and Fig. S2.

2.3 Sample analysis

Concentrations of dissolved organic carbon (DOC), total dissolved nitrogen (TDN), and dissolved inorganic nitrogen (DIN, including nitrite (NO_2^-), nitrate (NO_3^-), and ammonium (NH_4^+)) were measured using a TOC analyzer (multi N/C 3100, Analytik Jena) and a UV-Vis spectrophotometer (TU-1901, Persee), respectively (Ye et al., 2018; Wu et al., 2023). DON was calculated as the difference between TDN and DIN. The same procedures were used to determine nitrogen concentrations in the truly dissolved fraction (<1 kDa), and CON was calculated by difference (DON - tDON), as detailed in the Text S1 (Yang et al., 2021). Particulate organic carbon (POC), particulate nitrogen (PN), and stable isotopes ($\delta^{13}C$, $\delta^{15}N$) were analyzed on an elemental analyzer-isotope ratio mass spectrometer (DELTA V Advantage, Thermo Fisher Scientific) after acid treatment to remove carbonates. Particulate inorganic nitrogen (PIN) was determined via HCl extraction (Zuo et al., 2016) and accounted for less than 5% of total PN in all samples; therefore, PN was used as a proxy for PON. The potential influence of PIN on $\delta^{15}N$-PON was further evaluated using an isotope mass-balance sensitivity analysis, which indicated that the low PIN contribution would have only a minor effect on bulk $\delta^{15}N$ values and would not alter the observed isotopic trends (Text S2). All analyses were performed in triplicate. Measurement uncertainties from subtractions were estimated

using error propagation (Cornell et al., 2003). Further details on analytical precision, detection limits, and quality control are provided in Text S3.

Purified colloidal fraction (1 kDa–0.45 μm) and truly dissolved fraction (< 1 kDa) water samples (3 mL aliquots) were transferred to 1-cm quartz cuvettes for optical characterization using a UV-Vis spectrophotometer (TU-1901, Persee, China) and a fluorescence spectrometer (FS5, Edinburgh Instruments, UK). EEM fluorescence spectra were recorded across excitation wavelengths of 200–500 nm (5 nm intervals) and emission wavelengths of 250–700 nm (2 nm intervals), with a fixed spectral bandwidth of 5 nm. Milli-Q water blanks were analyzed regularly to ensure instrument stability. Optical indices, including the fluorescence index (FI), biological index (BIX), and specific UV absorbance at 254 nm ($SUVA_{254}$), were calculated from the corrected EEM fluorescence and UV–Vis absorbance spectra. FI and BIX were derived from fluorescence intensity ratios at specific excitation/emission wavelengths, whereas $SUVA_{254}$ was calculated by normalizing UV absorbance at 254 nm to the DOC concentration of the corresponding sample or fraction. Detailed equations and interpretations are provided in Text S4.

Additional water quality parameters including salinity, pH, SPM, and chlorophyll-a (Chl-a) were measured. The chemical composition of DON was analyzed using Fourier-transform infrared spectroscopy (FTIR, Nicolet iS10, Thermo Fisher Scientific, USA) after freeze-drying. Particle size distribution, polydispersity index (PdI), and zeta potential of the 0.45 μm-filtered filtrates were measured using a Zetasizer Nano ZS90 (Malvern Instruments, UK) at 25 °C. Activities of enzymes related to denitrification and organic matter degradation (nitrite reductase (NIR), succinate dehydrogenase (SDH), and chitinase (CHI); Solarbio, China) were quantified using commercial assay kits. ATPase activity was also measured with a commercial kit (Solarbio, China) to verify the effectiveness of chloroform-induced biological inhibition (Fig. S3a). Potential physicochemical interference from chloroform was assessed by monitoring particle properties in a separate control experiment. Zeta potential analysis showed no significant changes in average particle size, zeta potential, or PdI following chloroform addition (Fig. S3, $p > 0.05$), indicating minimal interference in the observed ON behavior during the experiments.

2.4 Statistical analyses

Statistical analyses were performed using IBM SPSS 20.0, with results presented as mean ± standard deviation ($n = 3$). Prior to one-way ANOVA, the normality of data distribution was assessed using the Shapiro–Wilk test, and homogeneity of variance was evaluated using Levene's test. Group differences were assessed by one-way ANOVA followed by Tukey's post hoc tests when the assumptions of normality and equal variance were satisfied. Conservative mixing was evaluated using a two-end-member mixing model based on the river-water and seawater endmembers to distinguish simple physical dilution from internal sources or sinks (Liss, 1976; Langmuir et al., 1978). The theoretical conservative concentration at each salinity was calculated as:

$$X_{mix} = f_r \times X_r + f_s \times X_s \quad (1)$$

$$f_r = (S_s - S_i) / (S_s - S_r),\ f_s = (S_i - S_r) / (S_s - S_r) \quad (2)$$

where X_{mix} was the predicted value under conservative mixing, X_r and X_s were the corresponding values in the river-water and seawater endmembers, respectively, f_r *and* f_s were the corresponding mixing fractions estimated from salinity, S_i, S_r, and S_s represent the salinity of the mixture, river-water endmember, and seawater endmember, respectively, and X represented nitrogen concentrations and PARAFAC component fluorescence intensities. Deviations between the observed value and the conservative mixing value (X_{mix}) were used to identify non-conservative behavior. The calculated theoretical values and deviations from conservative mixing for nitrogen concentrations and PARAFAC component fluorescence intensities were provided in Tables S3 and S4, respectively. Positive deviations were interpreted as net addition, whereas negative deviations were interpreted as net removal. Thus, a monotonic decrease in concentration with increasing salinity was not necessarily considered conservative unless the observed values followed the theoretical conservative mixing curve. PARAFAC was conducted in MATLAB (R2018b) using the DOMFluor toolbox (Stedmon and Bro, 2008). Spectra were corrected for inner-filter effects and Raman normalized following Murphy et al. (2010). A three-component model was selected based on residual analysis and split-half validation. Component fluorescence intensity was normalized to the total intensity per sample. Relationships between parameters were evaluated using regression analysis. A significance level of $p < 0.05$ was used for all tests.

3 Results

3.1 DON in estuarine mixing

DON, comprising tDON and CON, was the dominant form of ON under both mixing conditions, accounting for over 71% of total ON, with CON contributing 19–41% (Fig. S4). Along the increasing salinity gradient, the concentrations of CON, tDON, and PON all declined (Fig. 1; Table S2); however, DON decreased proportionally more than PON, causing the relative contribution of DON to total ON to decline while that of PON increased (Fig. S4). Conservative mixing was evaluated by comparing the observed concentrations with the theoretical two-end-member dilution curves shown as solid lines in Fig. 1. The observed tDON and CON concentrations deviated from the conservative mixing curve (Fig. 1; Table S3), indicating non-conservative behavior. Specifically, tDON showed significant addition in the BAM treatments and removal in the BIM treatments, while CON exhibited removal under both BAM and BIM treatments. A significant difference was thus observed by including and excluding biological processes between the two mixing treatments ($n = 21$, $p < 0.05$).

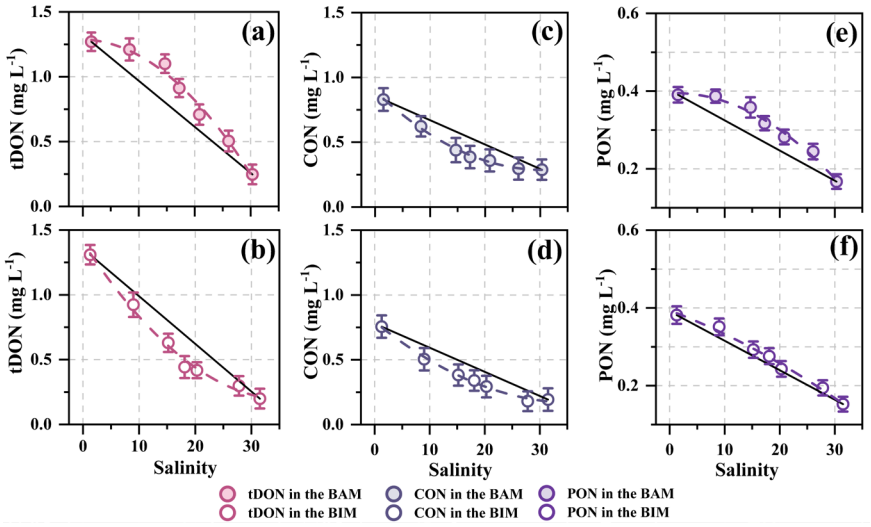

Figure 1. Variations in the concentrations of truly dissolved organic nitrogen (tDON) (a, b), colloidal organic nitrogen (CON) (c, d) and particulate organic nitrogen (PON) (e, f) across different river-seawater mixing ratios in the biologically active mixing (BAM) and biologically inhibited mixing (i.e., physicochemical mixing only, BIM) treatments. Conservative mixing curves (solid lines) were calculated using a two-end-member model based on the river-water and seawater endmembers (Langmuir et al., 1978), while dashed lines represent smoothed fits to the observed data. Deviations of the observed data from the conservative mixing curves indicate non-conservative behavior, with positive deviations representing net addition and negative deviations representing net removal.

PARAFAC analysis identified the three fluorescent components (Fig. 2; Table S5) commonly observed in natural DOM: two humic-like components (C1: terrestrial; C3: microbial) and one protein-like component (C2). All components decreased with increasing salinity (Fig. S5; Table S2), yet showed distinct non-conservative behaviors. C2 and C3 were particularly influenced by biological processes. Compared with the theoretical fluorescence values calculated using the same two-end-member conservative mixing model as for nitrogen concentrations, all three components showed negative deviations in the BIM treatments (Fig. 2; Table S4). In contrast, in the BAM treatments, C1 and C3 showed negative deviations, whereas C2 showed positive deviation, indicating net addition of protein-like fluorescence under biologically active conditions (Fig. 2; Table S4). Optical indices of DON also varied along the salinity gradient (Fig. 3a–d). In all treatments, the fluorescence index (FI) and biological index (BIX) increased with rising salinity (Fig. 3a, c), while the specific UV absorbance at 254 nm ($SUVA_{254}$) decreased (Fig. 3b). FTIR spectra of the BAM treatments revealed an increase in amide-related absorption peaks (N–H and C=O stretching) and a decrease in humic-associated nitro group ($–NO_2$) signals with increasing salinity (Fig. 3d).

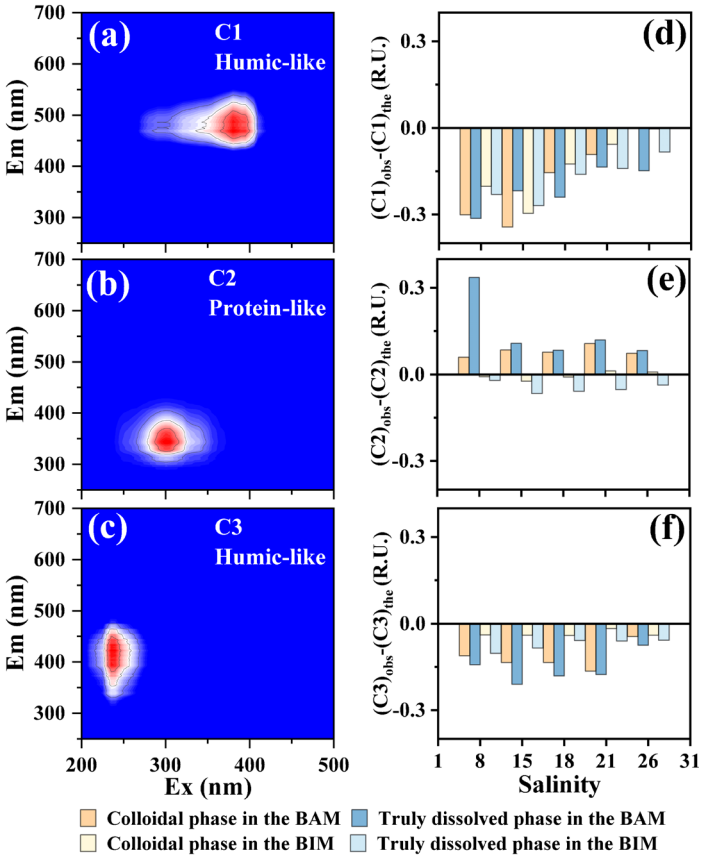

Figure 2. Variations in dissolved organic nitrogen (DON) components in the biologically active mixing (BAM) and biologically inhibited mixing (i.e., physicochemical mixing only, BIM) treatments. Panels a–c show the three fluorescence components identified by parallel factor analysis (PARAFAC): C1 - terrestrial humic-like ON, C2 - microbial protein-like ON, and C3 - microbial humic-like ON. Panels d–f display the difference in relative fluorescence intensity of C1, C2, and C3, respectively, plotted against salinity. These differences are calculated as the observed values ("obs") under mixed salinity conditions minus the theoretical values ("the") predicted by the two-end-member model. All Y-axis values in d–f are expressed in arbitrary units (R.U.), corrected using water Raman normalization.

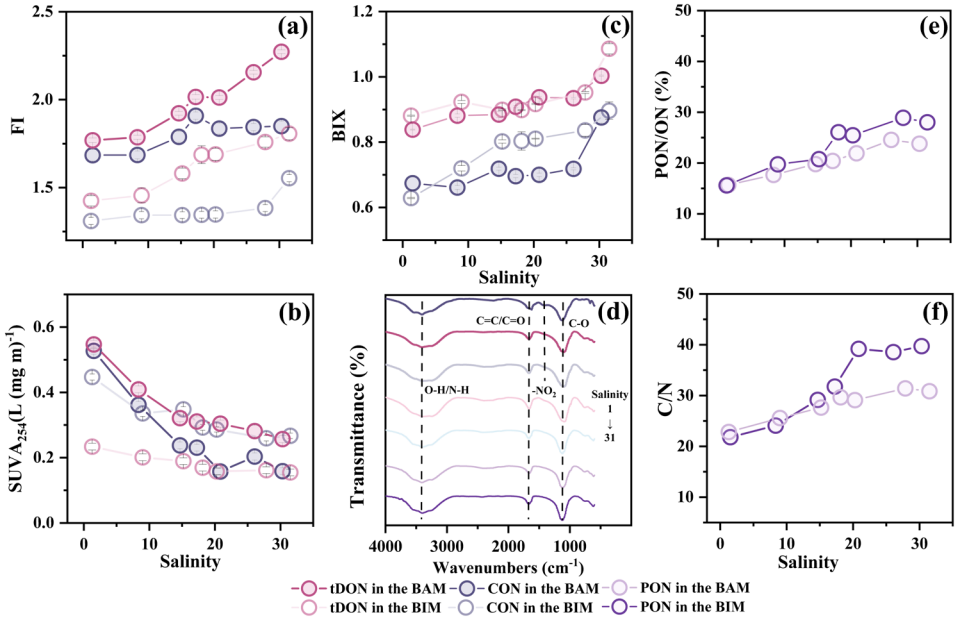

Figure 3. Changes in the compositions of dissolved organic nitrogen (DON) and particulate organic nitrogen (PON) along the salinity gradient in the biologically active mixing (BAM) and biologically inhibited mixing (i.e., physicochemical mixing only, BIM) treatments. Panels a–d show variations in DON properties with increasing salinity: (a) Fluorescence Index (FI); (b) Specific UV absorbance at 254 nm ($SUVA_{254}$); (c) Biological Index (BIX); and (d) FTIR spectra (shown for the BAM treatments only). Panels e–f display changes in particulate organic carbon (POC) characteristics with increasing salinity: (e) POC content and (f) C/N ratios.

3.2 PON in estuarine mixing

PON showed contrasting behavior between the two treatments. In the BIM treatments, PON concentrations were comparatively closer to the conservative mixing curve, with only slight positive deviation. In contrast, PON in the BAM treatments showed substantial positive deviation from the conservative mixing curve (Fig. 1e, f). Therefore, PON was not described as conservative under both treatments; rather, it behaved more conservatively in BIM than in BAM. Moreover, the proportion of PON and C/N ratio increased with rising salinity in both BAM and BIM treatments (Fig. 3e, f). In the BAM treatments, $\delta^{13}C$ and $\delta^{15}N$ of PON ranged from −28.3‰ to −26.5‰, and 1.1‰ to 8.8‰, respectively. While in the BIM treatments, $\delta^{13}C$ and $\delta^{15}N$ ranged from −26.1‰ to −25.9‰, and 6.2‰ to 7.2‰, respectively (Fig. 4a, b; Table S2). The salinity-related decrease in PON isotope values was mainly evident in the BAM treatments, whereas isotope variations in the BIM treatments were relatively small or non-monotonic. Specifically, both $\delta^{13}C$ and $\delta^{15}N$ values varied significantly among salinity levels as shown by one-way ANOVA ($p < 0.001$). Linear regression analysis based on the mean values at each salinity level further showed significant decreasing trends with increasing salinity for both $\delta^{13}C$-PON and $\delta^{15}N$-PON in the BAM treatments ($p < 0.001$, Fig. S7). In the BIM treatments, the regression analysis indicated only a weak decrease in $\delta^{13}C$-

PON with salinity (p = 0.039, Fig. S7), while δ^{15}N-PON showed no significant linear trend (p = 0.104, Fig. S7). Moreover, a significant positive correlation was also observed between the values of δ^{13}C-PON and δ^{15}N-PON (BAM: r = 0.93, p < 0.001; BIM: r = 0.63, p < 0.001; Fig. S7). The δ^{15}N values in this study were within the range reported in previous studies (Dong et al., 2022; Zhu et al., 2021).

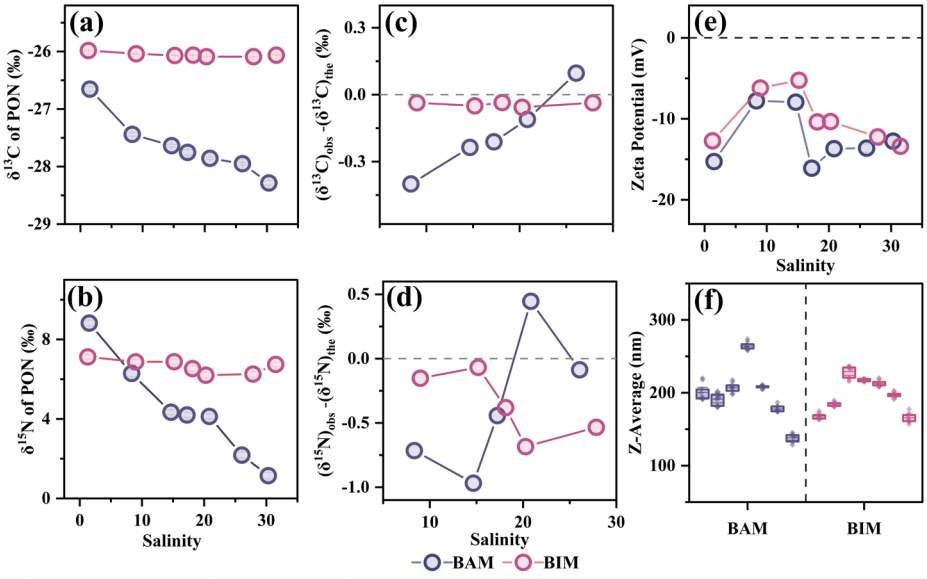

Figure 4. Variations of δ^{13}C values of particulate organic nitrogen (PON) (a), δ^{15}N values of PON (b), zeta potential (e), and mean particle size (f) along the salinity gradient in the biologically active mixing (BAM) and biologically inhibited mixing (i.e., physicochemical mixing only, BIM) treatments. Panels c and d show the deviations of δ^{13}C and δ^{15}N values of PON, respectively, calculated as the difference between the observed values ("obs") under mixed salinity conditions and the theoretical values ("the") predicted by the two-end-member model.

4 Discussion

4.1 Non-conservative behavior of organic nitrogen

The non-conservative behavior of DON during its transport from estuaries to the sea is primarily driven by a combination of biological activities and physicochemical interactions (Yan et al., 2022; Yan et al., 2024; Zhong et al., 2022). Adsorption, flocculation, and biological transformations of DON have been documented as important governing processes in major estuarine systems such as the Yangtze and Mississippi Rivers (Zhang et al., 2021; Zhou et al., 2021; Zhou et al., 2016). The non-conservative behavior of ON could be driven by two mechanistically distinct physicochemical processes under abiotic conditions (i.e., biologically inhibited mixing treatments). First, surface adsorption transferred DON onto SPM in the turbidity zone, where high SPM concentrations (Fig. S8b) provided abundant mineral surface area. This adsorption is

mediated primarily by non-electrostatic interactions, including ligand exchange, hydrogen bonding, and hydrophobic effects, between humic-like/aromatic DOM and mineral surfaces (Pan et al., 2020; Shimabuku et al., 2017; Yan et al., 2022), and is facilitated by the high proportion (>73%) of illite and quartz in the suspended matter (Table S1), which have a known affinity for aromatic DOM (Krettek et al., 2023). Second, increasing ionic strength along the salinity gradient compressed the electrical double layer of colloidal particles, driving zeta potential values toward neutrality (Fig. 4e). This reduction in electrostatic repulsion destabilized colloids, promoting particle aggregation and flocculation, as evidenced by the concurrent increase in mean particle size (Fig. 4f). The resulting aggregation facilitated the conversion of CON to PON. Additionally, the adsorption of LMW-DOM onto colloids (Kilduff et al., 1996; Pan et al., 2020) contributed to tDON removal, with efficiency dependent on DOM characteristics (Ateia et al., 2017) and properties of the colloidal material (Lee and Hur, 2016). In the absence of external ON inputs, the non-conservative ON behavior observed in the BIM treatments was primarily induced by salinity-driven flocculation and adsorption, resulting in dynamic exchanges between DON and PON pools. Importantly, the loss of CON during estuarine mixing implies that HMW fractions are preferentially removed from the dissolved phase by physicochemical processes (Fig. 1).

The contrasting DON dynamics between BAM and BIM treatments suggest the critical role of biological processes in estuarine DON transformation. In the BAM treatments, the removal of CON with a concurrent increase in tDON and PON (Fig. 1) aligns with observations in major global estuaries (Li et al., 2023; Thibodeau et al., 2017; Yan et al., 2022; Yan et al., 2024). This suggests that the active biological processing of DON is a widespread estuarine phenomenon, where DON serves as a key nitrogen source for microbial growth (Chen et al., 2022, 2024; Yan et al., 2024; Zhang et al., 2024). In our study, phytoplankton appeared to be involved in this transformation, as suggested by elevated Chl-a concentrations and their strong correlations with both PON formation and NO_3^- assimilation (Fig. S8). The preferential utilization of LMW-DON, consistent with previous findings in the region (Li et al., 2020; Zhang et al., 2024), further supports this conclusion. Since phytoplankton taxa exhibit varied preferences for inorganic nitrogen and ON substrates (Moschonas et al., 2017; Yan et al., 2022), DON availability becomes a critical factor in shaping community structure. This is particularly relevant for the Bohai Sea, where phytoplankton communities are reportedly shifting from NO_3^--preferring diatoms to DON-preferring dinoflagellates (Reinl et al., 2022; Chen et al., 2024a).

Microbial degradation is considered the dominant removal pathway for allochthonous DON input through estuaries to the Bohai Sea (Li et al., 2017). Although larger organic molecules require enzymatic hydrolysis for assimilation, HMW DON has been shown to degrade more rapidly than LMW fractions (Perliński and Mudryk, 2018), and to serve as a superior bacterial substrate (Li et al., 2020). In this study, NH_4^+ enrichment and elevated activities of SDH and CHI enzymes during the 3-day experimental period of the BAM treatments (Figs. S8e and S9b, c) further supported the biological reactivity of DON, particularly the CON fraction, indicating potential bacterial degradation pathways. These processes were likely promoted by DIN-depleted high-salinity conditions (Fig. S8). This is similar to patterns observed in the Elbe Estuary, where DON consumption and NH_4^+ regeneration occur concurrently (Schlarbaum et al., 2010). Overall, these results confirm that

estuarine DON exhibits non-conservative behavior driven by active biological processes, consistent with previous observations from the Yangtze (Yan et al., 2024) and Pearl River estuaries (Li et al., 2023).

4.2 Enhancement of DON bioavailability

The transformation of ON during estuarine mixing is governed by interacting factors such as the proportions of saltwater and freshwater, ON bioavailability, and particle characteristics, typically involving coupled biological and physicochemical mechanisms. The fluorescence EEM quantified compositional changes in DON across the estuarine mixing gradient (Fig. 2). Fig. S6 presents the statistical comparisons of deviations from conservative mixing. For the terrestrial humic-like component C1, ΔC1 values were negative in both treatments, indicating that measured C1 fluorescence intensities were lower than the theoretical conservative mixing values. The absence of a significant difference in ΔC1 between BAM and BIM treatments ($p > 0.05$; Fig. S6a) suggests that C1 attenuation relative to conservative mixing was mainly controlled by physicochemical processes, with limited additional biological influence (Shutova et al., 2014). In contrast, the significant differences ($p < 0.05$) in the behavior of the protein-like (C2) and microbial humic-like (C3) components between treatments reveal their susceptibility to both biological degradation and physicochemical interactions (Fig. S6b, c). Moreover, a strong positive correlation between DOC and DON ($n = 21$, $r > 0.97$, $p < 0.001$; Fig. S10a, b) indicates their coupling in the estuarine mixing processes. In the BAM treatments, accumulation of tDON was accompanied by increases in FI and BIX and a concurrent decrease in $SUVA_{254}$ (Fig. 3a–c). Because FI and BIX indicate microbial/autochthonous DOM contribution and recent biological production, respectively, whereas $SUVA_{254}$ reflects DOM aromaticity, these coordinated optical changes suggest an increased contribution of freshly produced, less aromatic DOM, supporting a shift toward greater potential DON bioavailability during estuarine mixing; direct uptake measurements would further constrain the extent to which this transformed DON pool is biologically utilized.

Physicochemical processes drive the significant non-conservative removal of humic-like components (C1 + C3), causing deviations of 10–21% from conservative mixing (Fig. 2). These abiotic processes alone accounted for the majority (63 ± 11%) of the total humic-like removal observed in the BAM treatments, with the refractory terrestrial component (C1) being a primary contributor. This finding aligns with observations in the Yangtze Estuary (Yan et al., 2024). Salt-induced flocculation during estuarine mixing is shown to remove both protein-like and humic-like components. HMW humic-like components (Asmala et al., 2014) are preferentially removed, consistent with the observed loss of CON (Fig. 1). Moreover, particulate matter, including colloids, adsorbs humic-like or aromatic DOM (Pan et al., 2020; Shimabuku et al., 2017; Yan et al., 2022), likely enhanced by the local mineralogy. The illite–quartz-dominated mineral matrix of SPM (Table S1), with its documented affinity for aromatic DOM (Krettek et al., 2023), likely explains the preferential transfer of humic-like components to the particulate phase. Therefore, particle adsorption and salt-induced flocculation were the dominant physicochemical removal pathways for humic-like DON.

In the BAM treatments, humic-like components (C1 + C3) showed similar removal trends as in the BIM treatments, but the fluorescence attenuation was greater, deviating more strongly from the theoretical dilution curve (Fig. 2, Table S2).

Conversely, the protein-like component (C2) increased significantly along the salinity gradient, opposite to its removal in the BIM treatments.

Strong correlations were observed between C2 and humic-like components (C1 + C3) in the BAM treatments ($n = 21$, $r = -0.95$, $p < 0.001$; Fig. S10c). C2 is a microbially derived protein-like component (Liu et al., 2024), C1 and C3 represent aromatic humic substances (Osburn et al., 2011), with C3 being more susceptible to microbial degradation (Cole et al., 2007; Yao et al., 2024). This inverse relationship is consistent with a pathway in which microbial degradation of humic-like substrates contributes to the production of labile, protein-like DON (Liu et al., 2024; Yao et al., 2024). However, this correlation alone does not prove direct transformation, and de novo microbial production of C2 using ambient DIN, labile DOC, or intracellular metabolites may also contribute to the observed pattern. Several independent lines of evidence support a predominantly transformative mechanism. Following a 3-day incubation, microbes consumed the ambient DOC and nutrients originally present in the riverine and marine waters to stimulate microbial growth and/or respiration, and change ON properties. Previous studies have shown that microbial activity, stimulated by terrestrial inputs, can transform humic-like components into shorter-wavelength humic or protein-like materials via a "priming effect" (Liu et al., 2024; Yao et al., 2024). Elevated expression of DON-degrading enzymes (SDH and CHI) in the BAM treatments (Fig. S9b, c) confirms active enzymatic processing of complex organic N, while concurrent NH_4^+ accumulation (Fig. S8e) is consistent with ammonification of humic-like substrates. These transformations were further supported by FTIR spectroscopy, in which the increase in amide-related peaks and decrease in humic-associated $–NO_2$ signals reflect partial removal of humic-like components and concurrent enrichment of protein-like material in the BAM treatments (Fig. 3d). Moreover, the strong correlation between microbial and terrestrial DON may imply that enhanced microbial metabolism accelerates DON degradation (Ward et al., 2016), especially in carboxylic acid- and heteroatom-rich fractions, and leads to the formation of labile DON (LDON, C2), which includes amino sugars, proteins, and lipids (Yao et al., 2024). This transformation pathway has previously also been documented in the Yangtze Estuary (Li et al., 2024). Taken together, the convergence of fluorescence, FTIR, enzymatic, and mass-balance evidence indicates that the observed inverse C2 – (C1 + C3) relationship is best explained by microbial transformation of humic-like DON into bioavailable LDON, potentially supplemented by de novo microbial synthesis. This process resulted in a relative increase in C2 fluorescence intensity of 6% to 12% above the theoretical dilution curve (Fig. 2, Table S2), leading to net tDON enrichment and enhanced overall DON potential bioavailability in the BAM treatments.

DON remained the dominant component of the ON pool (greater than 71%; Fig. S4), although its proportion decreased along the estuarine salinity gradient. As discussed above, the combined effects of physicochemical removal and biological degradation of humic-like components (C1 + C3) enhanced the relative abundance of the protein-like component (C2, LDON) within the residual pool. This processing also resulted in a net addition of tDON (LMW-DON), causing a positive deviation from the conservative two-end-member mixing model (Fig. 1). These observations demonstrate that the interplay between physicochemical and biological processes during estuarine mixing enhances the bioavailability of DON, especially its LMW fraction. These findings highlight the importance of biological processes in regulating DON recycling, further

demonstrating their dominant role in shaping the bioavailability of DON. The increased bioavailability of DON has implications for the size, stability, and reactivity of the dissolved nitrogen pool in estuarine and coastal systems, potentially affecting primary productivity and nitrogen retention capacity.

4.3 Accumulation of refractory PON

As discussed, PON content exceeded conservative mixing predictions in both treatments, with concurrent increases in C/N ratios (Fig. 3e, f). This increase in PON can be attributed to two main processes: (1) adsorption and flocculation of DON onto particulate matter, and (2) biological production of PON by planktonic organisms. Flocculation and particle adsorption predominantly target dissolved humic-like/aromatic components (C1 + C3, RDON), with the extent of removal influenced by ON composition, concentration, and interactions with mineral surfaces (Krettek et al., 2023). Field studies have shown that settling particles in dynamic sedimentation–resuspension systems can become coated with refractory organic matter (Liu et al., 2024; Roland et al., 2008), facilitating the accumulation of refractory PON in aquatic environments.

The isotopic deviations further constrain this mechanism by indicating that refractory PON accumulation involved the selective re-adsorption of microbially modified, ^{15}N-enriched RDON. In a simple dilution scenario, δ^{15}N-PON would be expected to decrease linearly toward the seawater end-member value. Phytoplankton assimilation of DIN may further lower δ^{15}N-PON through isotopic fractionation (Chen et al., 2024b). However, in the BAM treatments, both δ^{13}C and δ^{15}N exceeded the theoretical mixing predictions at intermediate salinities, with enrichments of +0.10‰ and +0.45‰, respectively (Fig. 4c, d). This indicates that a process introducing or retaining ^{15}N-enriched material in the PON pool must have operated and outweighed the opposing input of isotopically light phytoplankton-derived PON. ON modified by microbial activity, including microbial products and residues, tends to have a higher C/N ratio, more negative δ^{13}C values, and elevated δ^{15}N values. These isotopic shifts are known to result from fractionation during the biosynthesis of cellular components (Abraham and Hesse, 2003; Ogawa et al., 2001). Because phytoplankton DIN assimilation would tend to lower rather than raise δ^{15}N-PON, the observed positive deviations strongly implicate the selective re-adsorption of microbially modified, ^{15}N-enriched and residual refractory DON (RDON′) onto particles as the dominant mechanism. Several complementary observations support this interpretation. The increase in C/N ratios with salinity (Fig. 4f) suggests a shift toward microbially processed organic matter rather than fresh phytoplankton biomass, which typically has lower C/N ratios. In addition, free energy calculations have shown that microbial transformation products, such as amino sugars, are thermodynamically favored for adsorption onto particles (Liu et al., 2024). As no external particles were introduced during the mixing experiments, the net positive δ^{15}N deviation most likely reflects in-situ RDON′ adsorption and particle-phase retention, contributing to the accumulation of refractory, isotopically enriched ON in the particulate pool.

This study highlights that estuarine mixing processes significantly reshape the composition and quantity of PON mainly through biological modifications and adsorption and flocculation of refractory DON. These processes account for at least 44-71% of the removal of humic-like components. These transformation pathways result in particle-associated accumulation of refractory ON, a process often overlooked in studies of estuarine particle dynamics. Given rising anthropogenic ON inputs to

river–estuary systems (Yan et al., 2025), the relative proportion of PON within suspended particles is likely to increase further. Moreover, the biological and physicochemical characteristics of particle-associated ON, having undergone extensive degradation and interaction with mineral surfaces, may differ substantially from newly produced ON (Roland et al., 2008). This transformation process likely enhances the potential for ON burial during transport from river to the sea.

4.4 Mixing-driven organic nitrogen transformation and fate

Estuarine ON exhibits both conservative and non-conservative behavior during its transport to the sea (Fig. 5a, b), with variability driven to differing extents by biological and physicochemical processes. This study shows that salt-induced flocculation and adsorption during estuarine mixing preferentially removed ON, especially HMW humic-like components (C1 + C3), from the dissolved pool, transferring them to particulate phases and promoting the accumulation of refractory components (Fig. 6a, Pathway 1). In parallel, microbial utilization of terrestrial DOC and DON as a nutrient source enhanced biological activity, leading to degradation of humic-like components (C1 + C3) and subsequent enrichment of NH_4^+ and LMW-DON (tDON, Fig. 6b, Pathway 2), increasing the bioavailability of dissolved nitrogen. In turn, the selective re-adsorption process of refractory DON (RDON′) derived from microbial transformation onto particles further promotes the formation of particle-associated refractory nitrogen (Fig. 6c, Pathway 3).

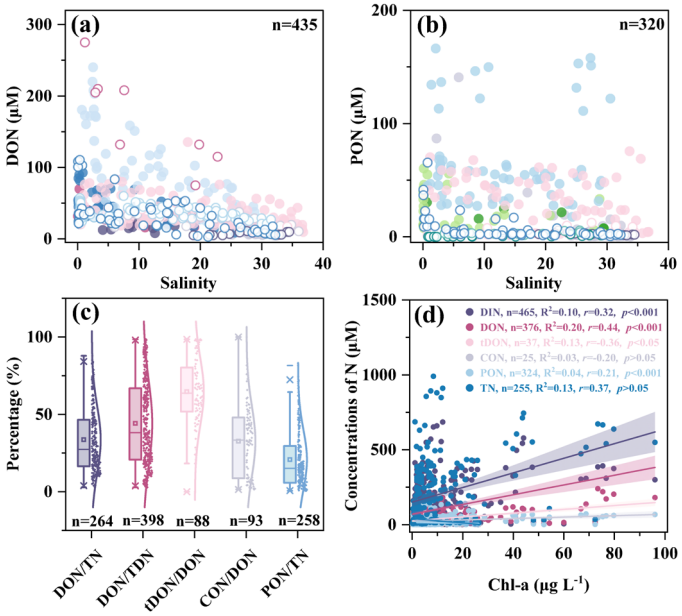

Figure 5. Non-conservative behavior of dissolved organic nitrogen (DON) (a) and particulate organic nitrogen (PON) (b) along the salinity gradient in estuarine mixing zones of rivers discharging into the global ocean. Different colors and symbols (hollow and solid) represent different estuaries; detailed site information is provided in Table S6. (c) Boxplots showing the proportions of DON and PON relative to total nitrogen (TN), DON relative to total dissolved nitrogen (TDN),

and the distribution of truly dissolved organic nitrogen (tDON) and colloidal organic nitrogen (CON) within DON. (d) Correlation analysis between organic nitrogen species and chlorophyll-a (Chl-a) concentrations in the water column.

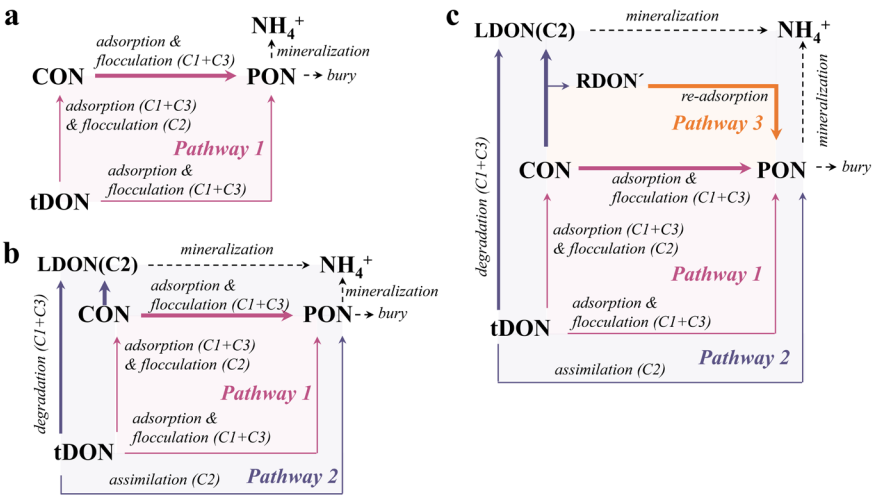

Figure 6. Conceptual pathways (1-3) illustrating the transformation of organic nitrogen (ON) during estuarine mixing. Pathway 1 (a): Adsorption and flocculation of humic-like (C1 + C3) and protein-like (C2) components from truly dissolved organic nitrogen (tDON) and colloidal organic nitrogen (CON) onto particulate phases. Pathway 2 (b): Microbial assimilation and degradation of DON, where DON serves as a carbon and nitrogen source, leading to the formation of labile DON (LDON), which may be mineralized or buried. Pathway 3 (c): Re-adsorption of refractory DON (RDON') generated or modified through microbial processes. The thick arrow represents the main pathways.

This study identifies a dual response during estuarine mixing: physicochemical removal of humic-like ON into refractory particulate pools and biological enhancement of residual DON bioavailability. This dual mechanism likely operates across estuaries worldwide, with relative intensities modulated by regional hydrodynamics, sediment characteristics, and the strength of coupled biological (microbial degradation, phytoplankton uptake) and physicochemical (adsorption/flocculation) processes. In physiochemically dominated estuaries, like the northern Gulf of Mexico (Zhou et al., 2016), ON transformation is mainly governed by dilution, flocculation, and sedimentary re-mineralization, leading to the transfer or burial of terrestrial nitrogen (Fig. 7a). However, biologically active estuaries operate differently. For example, humic-like components could be transformed into protein-like or inorganic nitrogen through microbial activity and enzymatic processes in the Yangtze Estuary (Yan et al., 2021; Yao et al., 2024), highlighting the significance of biologically mediated pathways (Fig. 7b, Pathway 2). The interplay of biological and physicochemical processes during mixing can produce compound effects. In the Pearl River Estuary, coupled mechanisms shape DON distribution (Li et al., 2023; Ye et al., 2018), while studies in the Yangtze Estuary have shown selective adsorption of microbially modified and 15N-enriched DON onto particles, supporting RDON′ burial (Chen et al., 2023; Yan et al., 2022; Zhou et al., 2021). Collectively, these findings, along with the results

from the current study, suggest that coupled biological and physicochemical interactions during mixing not only promote short-term ON transfer into the particulate phase through a top-down PON pump (Fig. 7b, Pathway 1 & 3), but also alter DON composition and bioavailability through biological activity (Fig. 7b, Pathway 2). Specifically, ON undergoing estuarine mixing is likely removed primarily through particle formation, the resulting PON may subsequently be buried or mineralized during transport. Nevertheless, DON remains the dominant fraction of the ON pool (greater than 71%) during DIN-depleted periods or under long residence times, and its modified forms may act as a nitrogen reservoir that could potentially fuel coastal algal blooms. Admittedly, this inference requires validation through in situ monitoring and bioassay experiments conducted in coastal waters.

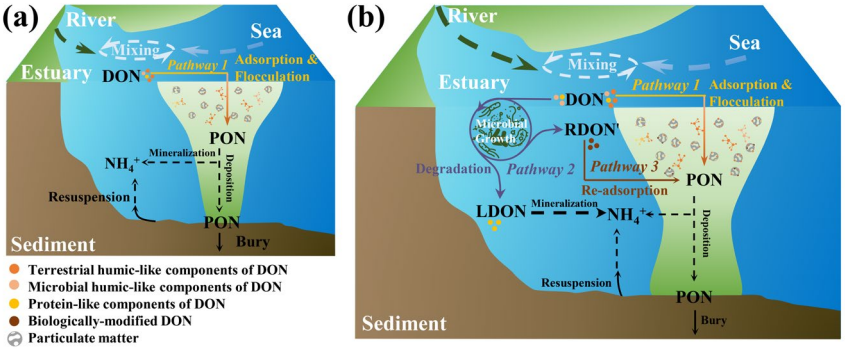

Figure 7. Conceptual model of nitrogen cycling under estuarine mixing, highlighting the role of organic nitrogen (ON) transformation. (a) Classical nitrogen pump model dominated by physicochemical processes, including dissolved organic nitrogen (DON) adsorption/flocculation, particulate organic nitrogen (PON) deposition and burial, resuspension, and mineralization. (b) Microbially enhanced nitrogen pump model, in which microbial utilization and transformation of terrestrial DON promote the degradation of humic-like DON, the production of NH_4^+ and labile DON (LDON), and the formation of microbially modified refractory DON (RDON′). The subsequent re-adsorption of RDON′ onto particles further promotes refractory PON accumulation and nitrogen retention during estuarine mixing.

Beyond the dual transformation mechanism itself, the resulting changes in ON composition have potential implications for downstream nitrogen bioavailability. Different ON forms contribute variably to TN, with marked variation in their composition and bioavailability (Fig. 5c). Changes in ON composition influence phytoplankton community structure, primary productivity, and the frequency of algal blooms (Hammer, 1993; Sethna and Royer, 2024; Zhang et al., 2024). For example, the increased availability of ON may lead to its transport into coastal waters, where it could serve as a supplementary nitrogen source, potentially elevating the risk of algal blooms. Such effects, if sustained at ecosystem scales, could cascade through food webs and alter the ecological stability and function of estuarine and coastal ecosystems (Atkinson et al., 2024). While TN is commonly used as a metric in eutrophication assessments (Browning and Moore, 2023), this study shows that Chl-a was more strongly correlated with DIN, DON, and tDON than with TN (Fig. 5d), indicating that nitrogen bioavailability, and thus eutrophication risk, is better predicted by nitrogen fractionation than by TN alone.

Furthermore, this study showed the increase of protein-like components during mixing, underscoring the importance of ON composition in regulating biological utilization. This suggests that both ON speciation and bulk composition could jointly affect its role in supporting productivity. The potential role of mixing-transformed ON in the increased frequency and distribution of algal blooms in coastal regions therefore deserves further investigation in future field studies.

4.5 Limitations and future perspectives

Several methodological constraints should be considered when extrapolating these results to natural estuaries. First, freshwater and seawater end-members were collected from a single summer sampling event (July 2024) and incubated under constant temperature and light, which does not capture the influence of multiple water sources (e.g., groundwater, tidal creek return flow, wastewater), tidal dynamics, stratification and resuspension cycles, or seasonal variability. Second, the 3-day incubation is sufficient to capture rapid flocculation, adsorption, and initial microbial transformation, but may underestimate slower processes such as long-term mineralization, sedimentation, and RDON' stabilization. Despite these constraints, the controlled two-end-member design allows us to disentangle rapid salinity-driven partitioning from concurrent biological processing, which are difficult to separate in the field, and provides a mechanistic baseline for interpreting non-conservative ON behavior along estuarine salinity gradients.

Future studies should extend incubation times and incorporate seasonal end-members to assess longer-term ON burial and the generality of these pathways beyond summer conditions. In particular, direct DON bioassays (e.g., isotope-labelled uptake experiments or microbial/phytoplankton growth bioassays) are needed to validate the inferred increases in DON bioavailability that were based on indirect optical and chemical proxies in this study. More broadly, establishing direct evidence linking mixing-induced ON transformations to downstream biological responses such as bloom initiation and trophic cascades would require seasonal field observations, mesocosm experiments, and coupled biogeochemical modelling. High-resolution molecular tools (e.g., FT-ICR MS, single-cell stable isotope analysis) should also be applied to resolve the full molecular diversity of DON transformations across estuarine gradients (Yan et al., 2024; Arandia-Gorostidi et al., 2024). It would further be valuable to integrate the salinity-dependent partitioning and biological conversion terms identified here into estuarine box or reactive-transport models, coupled with residence time and SPM properties, to generate quantitative predictions of ON export versus retention across estuary types.

5 Conclusions

This study reveals a dual response of organic nitrogen to estuarine mixing, in which physicochemical and biological processes simultaneously but differently reshape ON composition, bioavailability, and fate. The results show that physicochemical processes, specifically salt-induced adsorption and flocculation, act as a primary pathway for converting humic-like components of DON into refractory particulate forms, removing approximately 44–71% of humic-like DON (C1 + C3) and effectively creating a long-term sink. Crucially, isotopic evidence suggests that biologically modified DON re-

adsorbs onto particles, further enhancing their refractoriness. Concurrently, biological activity degrades the remaining labile humic-like fraction, releasing highly bioavailable nitrogen forms such as low-molecular-weight DON and NH_4^+ that fuel microbial production of protein-like substances, as reflected by an approximately 6–12% elevation in C2 fluorescence above conservative mixing predictions. These results highlight that the dual response of ON during estuarine mixing, characterized by refractory PON accumulation versus enhanced DON bioavailability, cannot be captured by bulk nitrogen metrics alone, underscoring the value of ON speciation in estuarine nitrogen assessments. Future research should test whether this dual mechanism generalizes across seasons and estuary types, and quantify how the balance between physicochemical and biological pathways modulates the bioavailability of ON exported to coastal waters.

Data availability

Data of nutrients and isotopes generated by this study can be found in the Supplement.

Supplement link

The supplement related to this article is available online at XXX.

Author contributions

CH led the study conceptualization and methodology, curated the data, produced the visualizations, and wrote the original draft; SQ contributed to methodology development; YK and XL curated the data; RDV contributed to manuscript review and editing; XL provided supervision and funding acquisition and contributed to manuscript review and editing.

Competing interests

The authors declare there are no conflicts of interest for this manuscript.

Disclaimer

Publisher's note: Copernicus Publications remains neutral with regard to jurisdictional claims made in the text, published maps, institutional affiliations, or any other geographical representation in this paper. The authors bear the ultimate responsibility for providing appropriate place names. Views expressed in the text are those of the authors and do not necessarily reflect the views of the publisher.

Financial support

This work was supported by the National Key R&D Program of China (Grant numbers: 2024YFF1306800).

Review statement

References

Abraham, W. R. and Hesse, C.: Isotope fractionations in the biosynthesis of cell components by different fungi: A basis for environmental carbon flux studies, FEMS Microbiol. Ecol., 46, 121–128, https://doi.org/10.1016/S0168-6496(03)00203-4, 2003.

Arandia-Gorostidi, N., Jaffe, A. L., Parada, A. E., Kapili, B. J., Casciotti, K. L., Salcedo, R. S. R., Baumas, C. M. J., and Dekas, A. E.: Urea assimilation and oxidation support activity of phylogenetically diverse microbial communities of the dark ocean, ISME J., 18, wrae230, https://doi.org/10.1093/ismejo/wrae230, 2024.

Asmala, E., Bowers, D. G., Autio, R., Kaartokallio, H., and Thomas, D. N.: Qualitative changes of riverine dissolved organic matter at low salinities due to flocculation, J. Geophys. Res.-Biogeo., 119, 1919–1933, https://doi.org/10.1002/2014JG002722, 2014.

Ateia, M., Apul, O. G., Shimizu, Y., Muflihah, A., Yoshimura, C., and Karanfil, T.: Elucidating adsorptive fractions of natural organic matter on carbon nanotubes, Environ. Sci. Technol., 51, 7101–7110, https://doi.org/10.1021/acs.est.7b01279, 2017.

Atkinson, A., Rossberg, A. G., Gaedke, U., Sprules, G., Heneghan, R. F., Batziakas, S., Grigoratou, M., Fileman, E., Schmidt, K., and Frangoulis, C.: Steeper size spectra with decreasing phytoplankton biomass indicate strong trophic amplification and future fish declines, Nat. Commun., 15, 381, https://doi.org/10.1038/s41467-023-44406-5, 2024.

Berman, T. and Bronk, D. A.: Dissolved organic nitrogen: A dynamic participant in aquatic ecosystems, Aquat. Microb. Ecol., 31, 279–305, https://doi.org/10.3354/ame031279, 2003.

Bronk, D. A., See, J. H., Bradley, P., and Killberg, L.: DON as a source of bioavailable nitrogen for phytoplankton, Biogeosciences, 4, 283–296, https://doi.org/10.5194/bg-4-283-2007, 2007.

Browning, T. J. and Moore, C. M.: Global analysis of ocean phytoplankton nutrient limitation reveals high prevalence of co-limitation, Nat. Commun., 14, 5014, https://doi.org/10.1038/s41467-023-40774-0, 2023.

Cai, W., Wiebe, W. J., Wang, Y., and Sheldon, J. E.: Intertidal marsh as a source of dissolved inorganic carbon and a sink of nitrate in the Satilla River-estuarine complex in the southeastern U.S., Limnol. Oceanogr., 45, 1743–1752, https://doi.org/10.4319/lo.2000.45.8.1743, 2000.

Chen, K., Li, K., Gao, P., Wang, P., Han, X., Chen, Y., and Wang, X.: Was dissolved nitrogen regime driving diatom to dinoflagellate shift in the bohai sea? Evidences from microcosm experiment and modeling reproduction, J. Geophys. Res.-Biogeo., 127, e2021JG006737, https://doi.org/10.1029/2021JG006737, 2022.

Chen, K., Yang, R., Li, M., Chen, Y., Han, X., Zhao, J., Li, K., and Wang, X.: The hydrophobic component of terrestrial dissolved organic nitrogen promotes shifting diatom–dinoflagellate dominance in the Bohai Sea, J. Geophys. Res.-Oceans, 129, e2024JC021373, https://doi.org/10.1029/2024JC021373, 2024a.

Chen, Y., Yang, J. Y. T., Tang, J., Hong, H., Kao, S. J., Dai, M., and Shi, D.: Changes in isotope fractionation during nitrate assimilation by marine eukaryotic and prokaryotic algae under different pH and CO_2 conditions, Limnol. Oceanogr., 69, 1045–1055, https://doi.org/10.1002/lno.12546, 2024b.

Chen, Z., Yi, Y., Zhang, H., Li, P., Wang, Y., Yan, Z., Wang, K., He, C., Shi, Q., and He, D.: Differences in dissolved organic matter molecular composition along two plume trajectories from the Yangtze River Estuary to the East China Sea, ACS Environ. Au, 4, 31–41, https://doi.org/10.1021/acsenvironau.3c00030, 2023.

Cole, J. J., Prairie, Y. T., Caraco, N. F., McDowell, W. H., Tranvik, L. J., Striegl, R. G., Duarte, C. M., Kortelainen, P., Downing, J. A., Middelburg, J. J., and Melack, J.: Plumbing the global carbon cycle: Integrating inland waters into the terrestrial carbon budget, Ecosystems, 10, 172–185, https://doi.org/10.1007/s10021-006-9013-8, 2007.

Cornell, S. E., Jickells, T. D., Cape, J. N., Rowland, A. P., and Duce, R. A.: Organic nitrogen deposition on land and coastal environments: a review of methods and data, Atmos. Environ., 37, 2173–2191, https://doi.org/10.1016/S1352-2310(03)00133-X, 2003.

Dähnke, K., Sanders, T., Voynova, Y., and Wankel, S. D.: Nitrogen isotopes reveal a particulate-matter-driven biogeochemical reactor in a temperate estuary, Biogeosciences, 19, 5879–5891, https://doi.org/10.5194/bg-19-5879-2022, 2022.

Dong, S., Wang, X. T., Subhas, A. V., Pavia, F. J., Adkins, J. F., and Berelson, W. M.: Depth profiles of suspended carbon and nitrogen along a North Pacific transect: Concentrations, isotopes, and ratios, Limnol. Oceanogr., 67, 247–260, https://doi.org/10.1002/lno.11989, 2022.

Edokpa, D. A., Evans, M. G., Boult, S., and Rothwell, J. J.: Size fractionation of dissolved organic nitrogen in peatland fluvial systems, Environ. Sci. Technol., 52, 11198–11205, https://doi.org/10.1021/acs.est.8b01417, 2018.

Fagerberg, T., Carlsson, P., and Lundgren, M.: A large molecular size fraction of riverine high molecular weight dissolved organic matter (HMW DOM) stimulates growth of the harmful dinoflagellate Alexandrium minutum, Harmful Algae, 8, 823–831, https://doi.org/10.1016/j.hal.2009.02.002, 2009.

Ghosh, V. R. D., Rajula, G. R., Kumar, B. S. K., and Sarma, V. V. S. S.: Isotopic composition of carbon and nitrogen of particulate organic matter in the Godavari Estuary: Seasonality in sources and processes, Estuaries Coasts, 47, 128–143, https://doi.org/10.1007/s12237-023-01264-0, 2024.

Guo, L. and Santschi, P. H.: Composition and cycling of colloids in marine environments, Rev. Geophys., 35, 17–40, https://doi.org/10.1029/96RG03195, 1997.

Hammer, K. D.: Do soluble organic nitrogen compounds cause unusual algal blooms in seawater?, Int. J. Hyg. Envir. Heal., 194, 321–341, 1993.

Hounshell, A. G., Peierls, B. L., Osburn, C. L., and Paerl, H. W.: Stimulation of phytoplankton production by anthropogenic dissolved organic nitrogen in a coastal plain estuary, Environ. Sci. Technol., 51, 13104–13112, https://doi.org/10.1021/acs.est.7b03538, 2017.

Hu, H. and Ren, H.: Can fluorescence spectrometry be used as a surrogate for predicting the dissolved organic nitrogen and its bioavailable portion in wastewater effluents?, Chemosphere, 164, 299–303, https://doi.org/10.1016/j.chemosphere.2016.08.080, 2016.

Jani, J. and Toor, G. S.: Composition, sources, and bioavailability of nitrogen in a longitudinal gradient from freshwater to estuarine waters, Water Res., 137, 344–354, https://doi.org/10.1016/j.watres.2018.02.042, 2018.

Kellerman, A. M., Dittmar, T., Kothawala, D. N., and Tranvik, L. J.: Chemodiversity of dissolved organic matter in lakes driven by climate and hydrology, Nat. Commun., 5, 3804, https://doi.org/10.1038/ncomms4804, 2014.

Kilduff, J. E., Karanfil, T., Chin, Y., and Weber, W. J.: Adsorption of natural organic polyelectrolytes by activated carbon: A size-exclusion chromatography study, Environ. Sci. Technol., 30, 1336–1343, https://doi.org/10.1021/es950547r, 1996.

Kodama, T., Nishimoto, A., Horii, S., Ito, D., Yamaguchi, T., Hidaka, K., Setou, T., and Ono, T.: Spatial and seasonal variations of stable isotope ratios of particulate organic carbon and nitrogen in the surface water of the Kuroshio, J. Geophys. Res.-Oceans, 126, e2021JC017175, https://doi.org/10.1029/2021JC017175, 2021.

Krettek, A., Höschen, C., Richter, G., Schweizer, S., and Rennert, T.: Retention of dissolved organic matter during podzolisation: Testing processes in laboratory experiments and at the submicron scale, Geoderma Reg., 32, e00606, https://doi.org/10.1016/j.geodrs.2023.e00606, 2023.

Langmuir, C. H., Vocke, R. D., Hanson, G. N., and Hart, S. R.: A general mixing equation with applications to Icelandic basalts, Earth Planet. Sci. Lett., 37, 380–392, https://doi.org/10.1016/0012-821X(78)90053-5, 1978.

Lee, B. M. and Hur, J.: Adsorption behavior of extracellular polymeric substances on graphene materials explored by fluorescence spectroscopy and two-dimensional fourier transform infrared correlation spectroscopy, Environ. Sci. Technol., 50, 7364–7372, https://doi.org/10.1021/acs.est.6b01286, 2016.

Li, J., Wu, Y., Jiang, Z., Liu, S., Ren, Y., Yang, J., Song, X., Huang, X., and He, D.: Terrestrial and biological activities shaped the fate of dissolved organic nitrogen in a subtropical river-dominated estuary and adjacent coastal area, J. Geophys. Res.-Oceans, 128, e2023JC019911, https://doi.org/10.1029/2023JC019911, 2023.

Li, J., Wu, Y., Yang, J., Li, P., Jiang, Z., Liu, S., and Huang, X.: Estuarine hydrodynamic processes driving the molecular changes of terrestrial dissolved organic nitrogen: From mixing to biological modification, Sci. Total Environ., 917, 170489, https://doi.org/10.1016/j.scitotenv.2024.170489, 2024.

Li, K., Ma, Y., Dai, A., and Wang, X.: Degradation dynamics and bioavailability of land-based dissolved organic nitrogen in the Bohai Sea: Linking experiment with modeling, Mar. Pollut. Bull., 124, 856–870, https://doi.org/10.1016/j.marpolbul.2017.02.033, 2017.

Li, K., Liu, C., Ma, Y., and Wang, X.: Land-based dissolved organic nitrogen dynamics and bioavailability in Jiaozhou Bay, China, Estuar. Coast. Shelf S., 220, 13–24, https://doi.org/10.1016/j.ecss.2019.02.045, 2019.

Li, M., Li, K., Chen, K., Liu, C., Ma, Y., and Wang, X.: Size-based bioavailability of land-based DON and its impact on eutrophication of Jiaozhou bay, Mar. Pollut. Bull., 152, 110898, https://doi.org/10.1016/j.marpolbul.2020.110898, 2020.

Liu, X., Lan, C., Zhu, L., Yan, C., Wang, N., Chen, H., Zheng, G., Che, Y., Yang, Z., and Bao, R.: Sediment resuspension as a driving force for organic carbon transference and rebalance in marginal seas, Water Res., 257, 121672, https://doi.org/10.1016/j.watres.2024.121672, 2024.

Ma, M., Zhang, H., Lauerwald, R., Ciais, P., and Regnier, P.: Estimating lateral nitrogen transfers over the last century through the global river network using a land surface model, Earth Syst. Dyn., 16, 841–867, https://doi.org/10.5194/esd-16-841-2025, 2025.

Mayorga, E., Seitzinger, S. P., Harrison, J. A., Dumont, E., Beusen, A. H. W., Bouwman, A. F., Fekete, B. M., Kroeze, C., and Van Drecht, G.: Global Nutrient Export from WaterSheds 2 (NEWS 2): Model development and implementation, Environ. Model. Softw., 25, 837–853, https://doi.org/10.1016/j.envsoft.2010.01.007, 2010.

Moschonas, G., Gowen, R. J., Paterson, R. F., Mitchell, E., Stewart, B. M., McNeill, S., Glibert, P. M., and Davidson, K.: Nitrogen dynamics and phytoplankton community structure: the role of organic nutrients, Biogeochemistry, 134, 125–145, https://doi.org/10.1007/s10533-017-0351-8, 2017.

Murphy, K. R., Butler, K. D., Spencer, R. G. M., Stedmon, C. A., Boehme, J. R., and Aiken, G. R.: Measurement of dissolved organic matter fluorescence in aquatic environments: An interlaboratory comparison, Environ. Sci. Technol., 44, 9405–9412, https://doi.org/10.1021/es102362t, 2010.

Officer, C. B.: Discussion of the behaviour of nonconservative dissolved constituents in estuaries, Estuar. Coast. Mar. Sci., 9, 91–94, https://doi.org/10.1016/0302-3524(79)90009-4, 1979.

Ogawa, H., Amagai, Y., Koike, I., Kaiser, K., and Benner, R.: Production of refractory dissolved organic matter by bacteria, Science, 292, 917–920, https://doi.org/10.1126/science.1057627, 2001.

Osburn, C. L., Wigdahl, C. R., Fritz, S. C., and Saros, J. E.: Dissolved organic matter composition and photoreactivity in prairie lakes of the U.S. Great Plains, Limnol. Oceanogr., 56, 2371–2390, https://doi.org/10.4319/lo.2011.56.6.2371, 2011.

Pan, J., Fu, X., Wang, C., Song, N., Lv, X., and Xu, H.: Adsorption and molecular weight fractionation of dissolved organic matters with different origins on colloidal surface, Chemosphere, 261, 127774, https://doi.org/10.1016/j.chemosphere.2020.127774, 2020.

Perliński, P. and Mudryk, Z. J.: Enzymatic biodegradation of high molecular weight polymers in the sediment–water interface in the coastal river estuary, River Res. Appl., 34, 745–754, https://doi.org/10.1002/rra.3308, 2018.

Reinl, K. L., Harris, T. D., Elfferich, I., Coker, A., Zhan, Q., De Senerpont Domis, L. N., Morales-Williams, A. M., Bhattacharya, R., Grossart, H. P., North, R. L., and Sweetman, J. N.: The role of organic nutrients in structuring freshwater phytoplankton communities in a rapidly changing world, Water Res., 219, 118573, https://doi.org/10.1016/j.watres.2022.118573, 2022.

Roland, L. A., McCarthy, M. D., and Guilderson, T.: Sources of molecularly uncharacterized organic carbon in sinking particles from three ocean basins: A coupled $\delta^{14}C$ and $\delta^{13}C$ approach, Mar. Chem., 111, 199–213, https://doi.org/10.1016/j.marchem.2008.05.010, 2008.

Rostad, C. E., Leenheer, J. A., and Daniel, S. R.: Organic carbon and nitrogen content associated with colloids and suspended particulates from the Mississippi River and some of its tributaries, Environ. Sci. Technol., 31, 3218–3225, https://doi.org/10.1021/es970196b, 1997.

Schlarbaum, T., Daehnke, K., and Emeis, K.: Turnover of combined dissolved organic nitrogen and ammonium in the Elbe estuary/NW Europe: Results of nitrogen isotope investigations, Mar. Chem., 119, 91–107, https://doi.org/10.1016/j.marchem.2009.12.007, 2010.

Schneider, A. B., Koschinsky, A., Kiprotich, J., Poehle, S., and Do Nascimento, P. C.: An experimental study on the mixing behavior of Ti, Zr, V and Mo in the Elbe, Rhine and Weser estuaries, Estuar. Coast. Shelf Sci., 170, 34–44, https://doi.org/10.1016/j.ecss.2015.12.002, 2016. Seitzinger, S. P., Sanders, R. W., and Styles, R.: Bioavailability of DON from natural and anthropogenic sources to estuarine plankton, Limnol. Oceanogr., 47, 353–366, https://doi.org/10.4319/lo.2002.47.2.0353, 2002.

Sethna, L. R. and Royer, T. V.: Response of dissolved organic matter to variation in nutrient availability and phytoplankton community composition in a mesotrophic, temperate-zone reservoir, Freshwater Sci., 43, 412–426, https://doi.org/10.1086/732260, 2024.

Shimabuku, K. K., Kennedy, A. M., Mulhern, R. E., and Summers, R. S.: Evaluating activated carbon adsorption of dissolved organic matter and micropollutants using fluorescence spectroscopy, Environ. Sci. Technol., 51, 2676–2684, https://doi.org/10.1021/acs.est.6b04911, 2017.

Sholkovitz, E. R.: Flocculation of dissolved organic and inorganic matter during the mixing of river water and seawater, Geochim. Cosmochim. Acta, 40, 831–845, https://doi.org/10.1016/0016-7037(76)90035-1, 1976.

Shutova, Y., Baker, A., Bridgeman, J., and Henderson, R. K.: Spectroscopic characterisation of dissolved organic matter changes in drinking water treatment: From PARAFAC analysis to online monitoring wavelengths, Water Res., 54, 159–169, https://doi.org/10.1016/j.watres.2014.01.053, 2014.

Stedmon, C. A. and Bro, R.: Characterizing dissolved organic matter fluorescence with parallel factor analysis: a tutorial, Limnol. Oceanogr. Methods, 6, 572–579, https://doi.org/10.4319/lom.2008.6.572, 2008.

Stedmon, C. A. and Markager, S.: Resolving the variability in dissolved organic matter fluorescence in a temperate estuary and its catchment using PARAFAC analysis, Limnol. Oceanogr., 50, 686–697, https://doi.org/10.4319/lo.2005.50.2.0686, 2005.

Tang, W., Fortin, S. G., Intrator, N., Lee, J. A., Kunes, M. A., Jayakumar, A., and Ward, B. B.: Determination of site-specific nitrogen cycle reaction kinetics allows accurate simulation of in situ nitrogen transformation rates in a large North American estuary, Limnol. Oceanogr., 69, 1757–1768, https://doi.org/10.1002/lno.12628, 2024.

Tang, W., Fortin, S. G., Intrator, N., Lee, J. A., Kunes, M. A., Jayakumar, A., Haynes, S. J., Oleynik, S., Sigman, D. M., and Ward, B. B.: Similar oxygen sensitivities of different steps of denitrification in estuarine waters, Environ. Sci. Technol., 59, 7165–7175, https://doi.org/10.1021/acs.est.5c02248, 2025.

Thibodeau, B., Bauch, D., and Voss, M.: Nitrogen dynamic in Eurasian coastal Arctic ecosystem: Insight from nitrogen isotope, Global Biogeochem. Cycles, 31, 836–849, https://doi.org/10.1002/2016GB005593, 2017.

Tivig, M., Keller, D. P., and Oschlies, A.: Riverine nitrogen supply to the global ocean and its limited impact on global marine primary production: a feedback study using an Earth system model, Biogeosciences, 18, 5327–5350, https://doi.org/10.5194/bg-18-5327-2021, 2021.

Wan, X., Sheng, H., Liu, L., Shen, H., Tang, W., Zou, W., Xu, M., Zheng, Z., Tan, E., Chen, M., Zhang, Y., Ward, B. B., and Kao, S.: Particle-associated denitrification is the primary source of N2O in oxic coastal waters, Nat. Commun., 14, 8280, https://doi.org/10.1038/s41467-023-43997-3, 2023.

Ward, N. D., Bianchi, T. S., Sawakuchi, H. O., Gagne-Maynard, W., Cunha, A. C., Brito, D. C., Neu, V., Valerio, A. de M., Silva, R. da, Krusche, A. V., Richey, J. E., and Keil, R. G.: The reactivity of plant-derived organic matter and the potential importance of priming effects along the lower Amazon River, J. Geophys. Res.-Biogeo., 121, 1522–1539, https://doi.org/10.1002/2016JG003342, 2016.

Wu, P., Gong, G., Cheng, J., Liu, K., and Kao, S.: Origins of particulate organic matter determined from nitrogen isotopic composition and C/N ratio in the highly eutrophic Danshuei Estuary, Northern Taiwan, Aquat. Geochem., 22, 291–311, https://doi.org/10.1007/s10498-016-9288-0, 2016.

Wu, Y., Li, J., Zhang, X., Jiang, Z., Liu, S., Yang, J., and Huang, X.: The distinct phases of fresh-seawater mixing intricately regulate the nitrogen transformation processes in a high run-off estuary: Insight from multi-isotopes and microbial function analysis, Water Res., 247, 120809, https://doi.org/10.1016/j.watres.2023.120809, 2023.

Xu, H., Lin, H., Jiang, H., and Guo, L.: Dynamic molecular size transformation of aquatic colloidal organic matter as a function of pH and cations, Water Res., 144, 543–552, https://doi.org/10.1016/j.watres.2018.07.075, 2018.

Yan, N., Qiu, Z., Zhang, C., Yan, Y., and Liu, D.: Landsat monitoring reveals the history of river organic pollution across China during 1984–2023, Water Res., 275, 123210, https://doi.org/10.1016/j.watres.2025.123210, 2025.

Yan, X., Yang, J., Xu, M., Wang, H., Dai, M., and Kao, S.: Nitrogen isotope constraint on the zonation of multiple transformations between dissolved and particulate organic nitrogen in the Changjiang plume, Sci. Total Environ., 818, 151678, https://doi.org/10.1016/j.scitotenv.2021.151678, 2022.

Yan, Z., Yang, N., Liang, Z., Yan, M., Zhong, X., Zhang, Y., Xu, W., and Xin, Y.: Active dissolved organic nitrogen cycling hidden in large river and environmental implications, Sci. Total Environ., 795, 148882, https://doi.org/10.1016/j.scitotenv.2021.148882, 2021.

Yan, Z., Xin, Y., Zhong, X., Yi, Y., Li, P., Wang, Y., Zhou, Y., Zhou, Y., He, C., Shi, Q., and He, D.: Dissolved organic nitrogen cycling revealed at the molecular level in the Bohai and Yellow Sea, Water Res., 244, 120446, https://doi.org/10.1016/j.watres.2023.120446, 2023.

Yan, Z., Xin, Y., Zhong, X., Yi, Y., Li, P., Wang, Y., Zhou, Y., He, Y., He, C., Shi, Q., Xu, W., and He, D.: Evolution of dissolved organic nitrogen chemistry during transportation to the marginal sea: Insights from nitrogen isotope and molecular composition analyses, Water Res., 249, 120942, https://doi.org/10.1016/j.watres.2023.120942, 2024.

Yang, B., Lin, H., Bartlett, S. L., Houghton, E. M., Robertson, D. M., and Guo, L.: Partitioning and transformation of organic and inorganic phosphorus among dissolved, colloidal and particulate phases in a hypereutrophic freshwater estuary, Water Res., 196, 117025, https://doi.org/10.1016/j.watres.2021.117025, 2021.

Yao, W., Dong, Y., Qi, Y., Han, Y., Ge, J., Volmer, D. A., Zhang, Z., Liu, X., Li, S., and Fu, P.: Tracking the changes of DOM composition, transformation, and cycling mechanism triggered by the priming effect: Insights from incubation experiments, Environ. Sci. Technol., 59, 430–442, https://doi.org/10.1021/acs.est.4c03784, 2024.

Ye, F., Guo, W., Wei, G., and Jia, G.: The sources and transformations of dissolved organic matter in the Pearl River Estuary, China, as revealed by stable isotopes, J. Geophys. Res.-Oceans, 123, 6893–6908, https://doi.org/10.1029/2018JC014004, 2018.

Zhang, G., Liang, S., Shi, X., and Han, X.: Dissolved organic nitrogen bioavailability indicated by amino acids during a diatom to dinoflagellate bloom succession in the Changjiang River estuary and its adjacent shelf, Mar. Chem., 176, 83–95, https://doi.org/10.1016/j.marchem.2015.08.001, 2015.

Zhang, X., Chen, S., Han, X., Su, R., Zhang, C., Liang, S., Yang, R., Wang, X., and Li, K.: Effects of organic nitrogen components from terrestrial input on the phytoplankton community in Jiaozhou Bay, Mar. Pollut. Bull., 174, 113316, https://doi.org/10.1016/j.marpolbul.2021.113316, 2022.

Zhang, X., Yu, K., Li, M., Jiang, H., Gao, W., Zhao, J., and Li, K.: Diatom-dinoflagellate succession in the Bohai Sea: The role of N/P ratios and dissolved organic nitrogen components, Water Res., 251, 121150, https://doi.org/10.1016/j.watres.2024.121150, 2024.

Zhang, Y., Ren, J., Zhang, W., and Wu, J.: Importance of salinity-induced stratification on flocculation in tidal estuaries, J. Hydrol., 596, 126063, https://doi.org/10.1016/j.jhydrol.2021.126063, 2021.

Zhong, X., Yan, M., Xu, W., Yan, Z., Xu, F., Dong, S., Xin, Y., and Shi, X.: Multiple lenses of N-isotopes reveal active dissolved organic nitrogen cycling in a subtropical estuary and marginal sea, Front. Mar. Sci., 9, 855479, https://doi.org/10.3389/fmars.2022.855479, 2022.

Zhou, J., Zheng, Y., Hou, L., An, Z., Chen, F., Liu, B., Wu, L., Qi, L., Dong, H., Han, P., Yin, G., Liang, X., Yang, Y., Li, X., Gao, D., Li, Y., Liu, Z., Bellerby, R., and Liu, M.: Effects of acidification on nitrification and associated nitrous oxide emission in estuarine and coastal waters, Nat. Commun., 14, 1380, https://doi.org/10.1038/s41467-023-37104-9, 2023.

Zhou, Y., He, D., He, C., Li, P., Fan, D., Wang, A., Zhang, K., Chen, B., Zhao, C., Wang, Y., Shi, Q., and Sun, Y.: Spatial changes in molecular composition of dissolved organic matter in the Yangtze River Estuary: Implications for the seaward transport of estuarine DOM, Sci. Total Environ., 759, 143531, https://doi.org/10.1016/j.scitotenv.2020.143531, 2021.

Zhou, Z., Stolpe, B., Guo, L., and Shiller, A. M.: Colloidal size spectra, composition and estuarine mixing behavior of DOM in river and estuarine waters of the northern Gulf of Mexico, Geochim. Cosmochim. Acta, 181, 1–17, https://doi.org/10.1016/j.gca.2016.02.032, 2016.

Zhu, J., Chen, M., Hu, W., Zheng, M., and Qiu, Y.: Biogeochemical cycling of nutrient in the western Bering Sea as revealed by nitrogen isotopic composition of nitrate and suspended particles, Deep-Sea Res. Pt. I, 174, 103551, https://doi.org/10.1016/j.dsr.2021.103551, 2021.

Zuo, J., Song, J., Yuan, H., Li, X., Li, N., and Duan, L.: Particulate nitrogen and phosphorus in the East China Sea and its adjacent Kuroshio waters and evaluation of budgets for the East China Sea Shelf, Cont. Shelf Res., 131, 1–11, https://doi.org/10.1016/j.csr.2016.11.003, 2016.